# Supplemental Information

## Whole-epigenome analysis in multiple myeloma reveals DNA hypermethylation of B cell-specific enhancers

***by Agirre et al.***

**Supplemental materials and methods**



**Supplemental figures**



**Supplemental Tables**

## Supplemental methods

### Patient samples

Bone marrow aspirations were performed after informed consent was obtained from newly diagnosed patients of MM (n=104), MGUS (n=16) and healthy donor samples of tonsil (n=8) and 4 pool samples of bone marrow of healthy donors (n=3). Both conventional karyotyping and FISH (Fluorescence in situ hybridization) were used to analyze the MM and MGUS. FISH analysis panel included IGH FISH probe, dual-color, dual-fusion translocation probes for t(4;14)(p16;q32) FGFR3/IGH, t(11;14)(q13;q32) CCND1/IGH, and t(14;16)(q32;q23) IGH/MAF and probes for deletion of 17p13.1 TP53 (LSI p53). Probes for detecting hyperdiploidy were designed for chromosomes 5, 9, and 15. The clinical and biological characteristics of the MM and MGUS patients selected for DNA methylation microarray analysis are shown in Supplemental Table 1. In all cases, the standards and recommendations of the Ethics Committee at the Hospital Universidad de Navarra and the declaration of Helsinki were followed.

### Isolation of plasma cells

To avoid possible confounding factors, the study was focused on purified plasma cells obtained from bone marrow aspirations or tonsils. The selection of plasma cells from bone marrow was made from the leukocyte fraction obtained after density gradient centrifugation. For MGUS and MM patient samples, when the baseline percentage of plasma cells in bone marrow was greater than 5%, we performed a positive selection by bead immunomagnetic selection with monoclonal mouse antihuman CD138+ antibodies using the AutoMACs Pro

separator automated system (Miltenyi Biotec, Germany). In contrast, for those cases where the percentage of CD138+ was within normal levels (~0.1%) in the bone marrow (e.g. control cases), after density gradient centrifugation we performed a selective depletion of CD3+, CD14+ and CD15+ cells by immunomagnetic selection (Miltenyi Biotec, Germany), followed by flow cytometry cell sorting of CD45+PerCP (Miltenyi Biotec, Germany)/CD138+PE (BD Biosciences, CA, USA)/CD38+FiTC (Miltenyi Biotec, Germany) cells using a FACSAriaII flow cytometer (BD Biosciences, CA, USA). Tonsillar plasma cells were separated from children tonsils obtained from the Clinica Universidad de Navarra (Pamplona, Spain). Tonsils were minced extensively and after Ficoll-Isopaque density centrifugation, enrichment of CD19+ cells was performed by using the AutoMACS system (Milteny Biotec, Auburn, CA). Plasma cells (CD20med/CD38high) were separated by FACS sorting after labeling with anti-CD20 FITC (BD Biosciences) and anti-CD38 APC (BD Biosciences).

In all cases, purity of the cell population was confirmed by 2-color flow cytometry using CD45+PerCP/CD138+ PE criteria (Miltenyi Biotec, Germany) and exceeded 90%. DNA and RNA were simultaneously obtained from the same sample using the Illustra triplePrep Kit (GE Healthcare), following manufacturer's instructions. DNA and RNA were quantified using a Nanodrop ND-100 spectrophotometer.

**U266 myeloma cell line**

MM cell line U266 was kindly provided by Dr. Cigudosa, Spanish National Cancer Centre (CNIO, Madrid, Spain). The U266 cell line was maintained in RPMI 1640, 20% of FBS and Penicilin/Streptomicin. The cell line was

maintained at 37$^{o}$C with 5% $CO_2$. The identity of the cell line was validated by using the Power Plex 1.2 System (Promega) and comparing the results to the Online STR Analysis Tool available at the DSMZ (http://www.dsmz.de/services/services-human-and-animal-cell-lines/online-str-analysis.html).

**Whole-genome bisulfite sequencing**

Genomic DNA (1-2µg) was spiked with unmethylated λ DNA (5ng of λ DNA per µg of genomic DNA) (Promega). The DNA was shared by sonication to 50-500bp using a Covaris E220 and fragments of size 150-300bp were selected using AMPure XP beads (Agencourt Bioscience Corp.). Genomic DNA libraries were constructed using the Illumina TruSeq Sample Preparation kit (Illumina Inc.) following the Illumina standard protocol: end repair was performed on the DNA fragments, an adenine was added to the 3' extremities of the fragments and Illumina TruSeq adapters were ligated at each extremity. After adaptor ligation, the DNA was treated with sodium bisulfite using the EpiTexy Bisulfite kit (Qiagen) following the manufacturer's instructions for formalin-fixed and paraffin-embedded (FFPE) tissue samples. Two rounds of bisulfite conversion were performed to assure a high conversion rate. Enrichment for adaptor-ligated DNA was carried out through 7 PCR cycles using the PfuTurboCx Hotstart DNA polymerase (Stratagene). Library quality was monitored using the Agilent 2100 BioAnalyzer (Agilent), and the concentration of viable sequencing fragments (molecules carrying adaptors at both extremities) estimated using quantitative PCR with the library quantification kit from KAPA Biosystem. Paired-end DNA sequencing (2x100bp) was then performed using the Illumina

Hi-Seq 2000. Amounts of sequence reads and the proportion of aligned reads are shown in Supplemental Table 2.

**Read mapping and estimation of cytosine methylation levels**

Read mapping was carried out using the GEM aligner (v1.242) (Marco-sola et al. 2012) against a composite reference containing two copies of the human GRCh37 reference and two copies of the NCBI viral genome database (v35). For both the human and viral references, one copy had all C bases replaced by T and the other had all G bases replaced by A. The names of the contigs in the combined reference FASTA file were modified by adding #C2T or #G2A to the end of the contig names depending on the conversion performed. Before mapping was performed the original sequence of each read was stored. The first read of each pair then had all C bases replaced by T, and the second read had all G bases replaced by A. Read mapping with GEM was performed allowing up to 4 mismatches per read from the reference. After read mapping the original sequence of each read was restored.

Estimation of cytosine levels was carried out on read pairs where both members of the read mapped to the same contig with consistent orientation, and there was no other such configuration at the same or less edit distance from the reference. After mapping, we restored the original read data in preparation for the inference of genotype and methylation status. We estimated genotype and DNA methylation status simultaneously using software developed at the Centro Nacional de Análisis Genómico, taking into account the observed bases, base quality scores and the strand origin of each read pair. For each genome position, we produced estimates of the most likely genotype and the methylation

proportion (for genotypes containing a C on either strand). A phred scaled likelihood ratio for the confidence in the genotype call was estimated for the called genotype at each position. For each sample, CpG sites were selected where both bases were called as homozygous CC followed by GG with a Phred score of at least 20, corresponding to an estimated genotype error level of <=1%. Sites with >500x coverage depth were excluded to avoid centromeric/telomeric repetitive regions. A common set of called CpG sites for all analyzed samples was generated, and all subsequent analyses used this common set.

**DNA methylation analysis with HumanMethylation450 BeadChip**

We used the EZ DNA Methylation Kit (Zymo Research) for bisulfite conversion of 500ng genomic DNA. Bisulfite-converted DNA was hybridized onto the HumanMethylation450 BeadChip kit (Illumina), which covers 99% of RefSeq genes and 96% of CpG islands. The Infinium methylation assay was carried out as described previously (Bibikova et al. 2011; Bibikova et al. 2009). Data from the HumanMethylation450 BeadChip were analyzed in R using the minfi package (version: 1.6.0) (*K. D. Hansen, M. Aryee. minfi: Analyze Illumina's 450k methylation arrays (2011))*, available through the Bioconductor open source software. To exclude technical and biological biases that might produce false results in further analyses, we developed and optimized an analysis pipeline with several filters (i.e. CpGs with low detection p values, sex-specific methylation or overlapping with SNPs). As NPCs from tonsils and bone marrow show some DNA methylation differences (Kulis et al. submitted), we also filtered out these differences and the consensus signature of NPC was used as normal

control of MM and MGUS samples. Taking into account the different performance of Infinium I and Infinium II assays we used the subset-quantile within array normalization (SWAN) (Maksimovic et al. 2012) that corrects for the technical differences between the Infinium I and II assay designs and produces a smoother overall beta value distribution. Unsupervised analyses were performed by principal component analysis (using only CpG sites with a SD above 0.2 among all samples) or hierarchical clustering using the Manhattan metric.

**Detection of differentially methylated regions**

The difference in methylation levels between each of the MM samples (M1 and M2) and normal plasma cells was calculated for all CpGs derived from the WGBS analysis. The normal approximation to the binomial was used to test for significant differences between samples. Hypo- or hypermethylated DMRs were defined as regions of consecutive CpG sites showing a consistent direction of methylation difference between a sample pair, with an average methylation absolute difference of ≥ 0.25. The maximum allowed distance between consecutive CpG sites inside a DMR was set to 150 bp.

For the high-density array data, we used the following criteria to define a consensus signature for MM or MGUS cases: a minimum absolute difference between mean DNA methylation values of cases and controls of at least 0.25 and a false discovery rate (FDR) of Wilcoxon tests for independent samples of less than 0.05.

**Annotation of CpG sites**

Both HumanMethylation450 BeadChip and WGSB data were annotated using data from the hg19 version of the UCSC Genome Browser. For the location relative to a gene, we used these categories: TSS 1500 (from 201 to 1,500 bp upstream of the transcriptional start site (TSS)), TSS 200 (from 1 to 200 bp upstream of the TSS), 5′ UTR, first exon, gene body (from the first intron to the last exon), 3′ UTR and intergenic regions. For the location relative to a CpG island (CGI), we used these groups: within CGI, in CGI shore (0–2 kb from the CGI edge), in CGI shelf (>2 kb to 4 kb from the CGI edge) and outside CGI. To study the association between DNA methylation and gene expression or chromatin states, we merged TSS 1500, TSS 200, 5′ UTR and first exon into a single category, called 5′ region. Also, gene body and 3′ UTR were merged into gene body. Owing to the presence of alternative transcription start sites and regions containing more than one gene, some of the CpGs were assigned multiple annotations.

We annotated all CpG probes using a recent categorization of chromatin and transcriptional states from the lymphoblastoid B cell line GM12878 (Ernst et al. 2011), which has a DNA methylome similar to memory B cells and plasma cells (Supplemental Fig. 7). Regions with chromatin states 1-2 (active and weak promoter) were considered as "Promoter regions", state 3 as "poised promoter", states 4-7 (strong and weak enhancer) as “Enhancer regions”, state 8 as "Insulator", states 9 and 10 (transcriptional transition and elongation) as "Strong transcription”, state 11 as "Weak transcription", state 12 as "Polycomb-repressed regions" and state 13 as "Heterochromatin (nuclear lamina)".

Replication timing in GM12878 data was obtained from the UW Repli-seq track of the UCSC Genome Browser (*http://genome.ucsc.edu/*).

The fold change enrichment of different chromatin states was calculated for hypo or hypermethylated CpGs as compared to the background distribution.

**Gene Ontology analysis**

The Gene Ontology enRIchment anaLysis and visuaLizAtion tool (GOrilla, http://cbl-gorilla.cs.technion.ac.il) was used to determine the enrichment of Gene Ontology terms in the groups of differentially methylated genes as compared with the 21,231 genes annotated with the HumanMethylation450 BeadChip (Eden et al. 2009).

**RNA-seq: alignment of Single-end Reads**

RNA samples from 11 MMs (also analyzed by HumanMethylation450 BeadChip) and 4 NPCs from tonsils were sequenced by the standard Illumina protocol to create raw sequence files (.fastq files), which underwent quality control analysis using FastQC (http://www.bioinformatics.babraham.ac.uk/projects/fastqc/). To avoid low quality data negatively influencing downstream analysis, we trimmed the reads on the 3′-end and only used the first 51 bp from the 5′-end of each read for further analysis. We aligned the quality checked reads to the Human Feb. 2009 (GRCh37/hg19) genome using TopHat version 2.0.9 allowing for unique alignments to the genome and up to two mismatches. The resulting alignments were summarized by Ensembl gene identifiers to evaluate number of uniquely aligned reads per transcript and per sample (raw read counts).

**Analysis of RNA-seq data**

RNA-seq data were analyzed using the limma package version 1.8.2 available through the Bioconductor open source. The raw read counts were used as input to form a DGEList object combining the counts and associated annotation. Transcripts with at least 1 count-per-million reads (cpm) in at least 7 samples were kept. Scale normalization was applied and the calculation of normalized signal was performed by voom function of the limma package (*C. W. Law, Y. Chen, W. Shi, G. K. Smyth. Voom! precision weightsunlock linear model analysis tools for RNA-seq read counts,* (*2013*)) available through the Bioconductor open source software. To study the association between gene expression and DNA methylation values of hypermethylated or hypomethylated CpGs, we linked data based on gene symbol and we calculated correlation coefficients. As the NPCs studied by RNA-seq and HumanMethylation450 BeadChip were not obtained from the same donors, the mean expression per gene (n=4 samples) and mean DNA methylation per CpG (n=8 samples) was used for correlation analysis.

**Luciferase Reporter Assay**

pCpGL empty vector and pCpGL-CMV/EF1 were kindly provided by Dr. Rehli, (University Hospital, Regensburg, Germany). To properly initiate the transcription, a CpG free minimal promoter (5´-AGAGGGTATATAATGGAAGCTTAACTTCCAG-3´) was also cloned in the pCpGL empty vector. We cloned enhancer regions of *SLC15A4*, *PVT1* and *NCOR2* genes, as defined by Ernst *et al*. (Ernst et al. 2011) in the GM12878

cell line, hypermethylated in MM samples compared to NPC controls. Amplicons ranged between 350-376 bp (Supplemental Table 5) were cloned into pCpGL-basic plus minimal promoter vector via BamHI and HindIII restriction sites. The correct insertion of all constructs was confirmed by direct sequencing. Constructions were in vitro methylated using SssI (New England Biolabs, Ipswich, Massachusetts), following manufacturer's recommendations. The in vitro methylation of all constructs was checked by bisulfite treatment followed by PCR and pyrosequencing (Supplemental Table 5).

All transfections were done using 2,5x105 HEK 293-T cells and harvested after 24 hours. As an internal transfection control we used a SV-40 Renilla reporter plasmid. Dual-Luciferase reporter system (Promega, Madison, Wisconsin) was used to measure the luminescent signal. All the transfections were done in triplicate and with duplicate measurements.

**Supplemental references**

Marco-Sola S, Sammeth M, Guigó R, Ribeca P. 2012. The GEM mapper: fast, accurate and versatile alignment by filtration. *Nat Methods* **9:** 1185-1188.

Bibikova M, Barnes B, Tsan C, Ho V, Klotzle B, Le JM, Delano D, Zhang L, Schroth GP, Gunderson KL, *et al.* 2011. High density DNA methylation array with single CpG site resolution. *Genomics* **98:** 288-295.

Bibikova M, Le J, Barnes B, Saedinia-Melnyk S, Zhou L, Shen R, Gunderson KL. 2009. Genome-wide DNA methylation profiling using Infinium assay. *Epigenomics* **1:** 177-200.

Maksimovic J, Gordon L, Oshlack A. 2012. SWAN: Subset-quantile within array normalization for illumina infinium HumanMethylation450 BeadChips. *Genome Biol* **13**: R44.

Ernst J, Kheradpour P, Mikkelsen TS, Shoresh N, Ward LD, Epstein CB, Zhang X, Wang L, Issner R, Coyne M, *et al.* 2011. Mapping and analysis of chromatin state dynamics in nine human cell types. *Nature* **473:** 43-49.

Eden E, Navon R, Steinfeld I, Lipson D, Yakhini Z. 2009. GOrilla: a tool for discovery and visualization of enriched GO terms in ranked gene lists. *BMC Bioinformatics* **10**: 48.

## Supplemental Figures

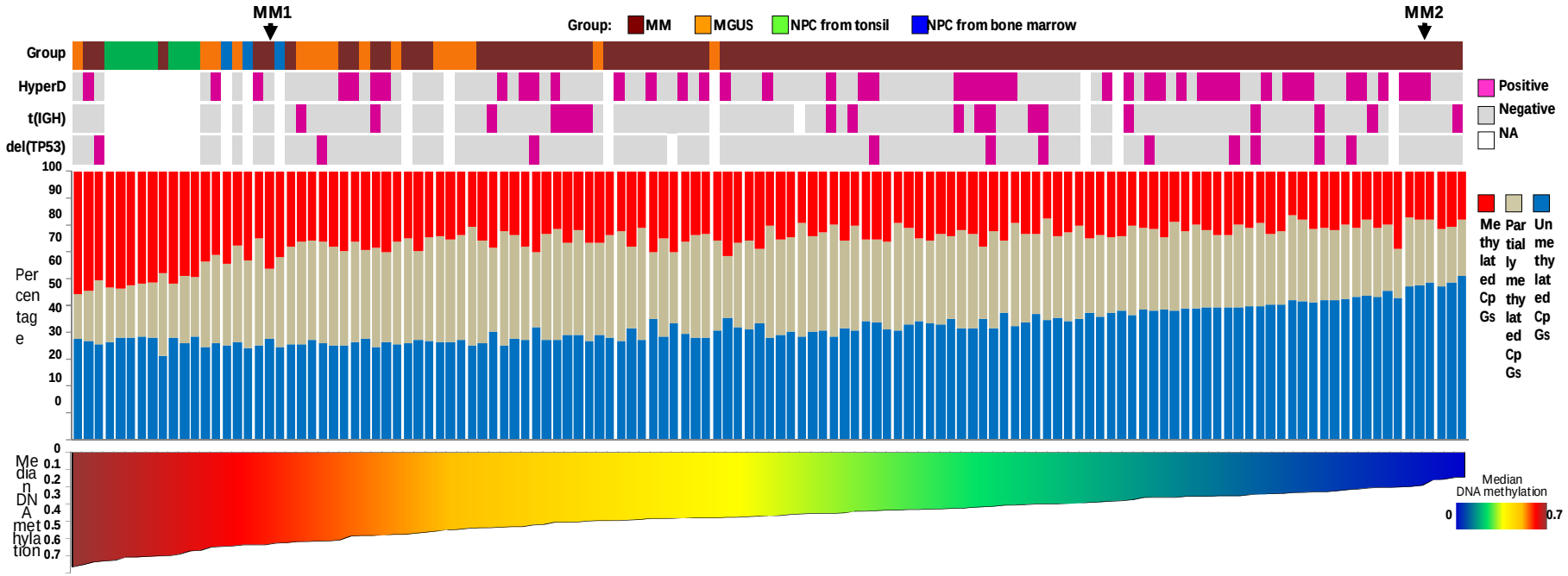


**Supplemental Fig. 1. DNA methylation patterns in MM, MGUS and normal plasma cells (NPC)**. Distribution of unmethylated (beta value ≤ 0.25), partially methylated (beta value between 0.25 and 0.75) and methylated (beta value ≥ 0.75) CpG sites using HumanMethylation450 BeadChip data from NPCs, MGUS and MM. Samples are arranged from higher to lower median methylation values (displayed at the bottom of the panel) and cytogenetic data is shown at the top of the panel. HyperD: hyperdiploid MM sample; t(IGH): MM sample with *IGH* translocation and del(TP53): MM sample with deletion of *TP53* gene.

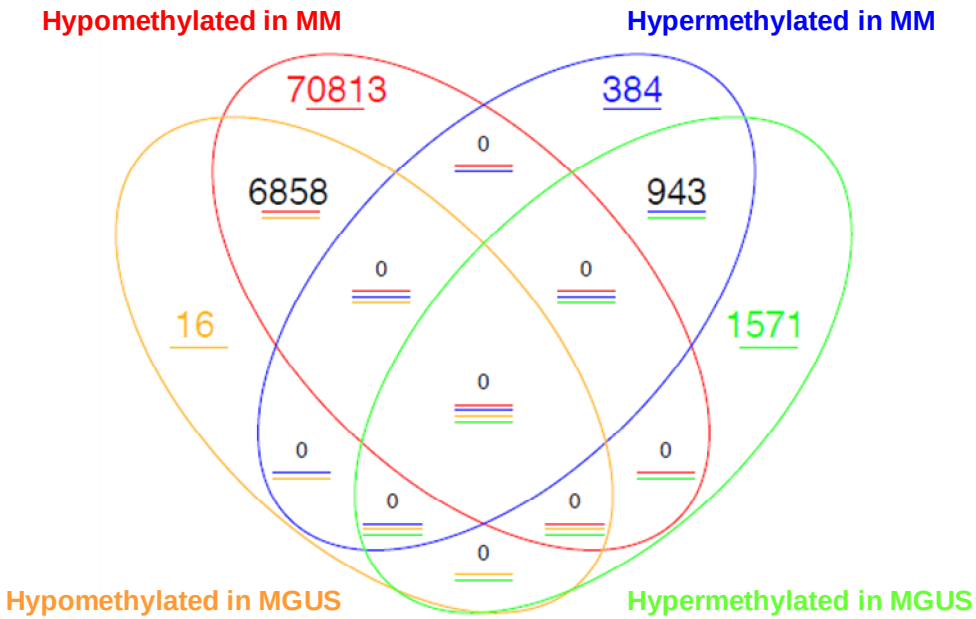


**Supplemental Fig. 2. DNA methylation in MM and MGUS as compared to NPCs.** Venn diagram with differentially DNA methylated CpGs in MGUS and MM patient samples.

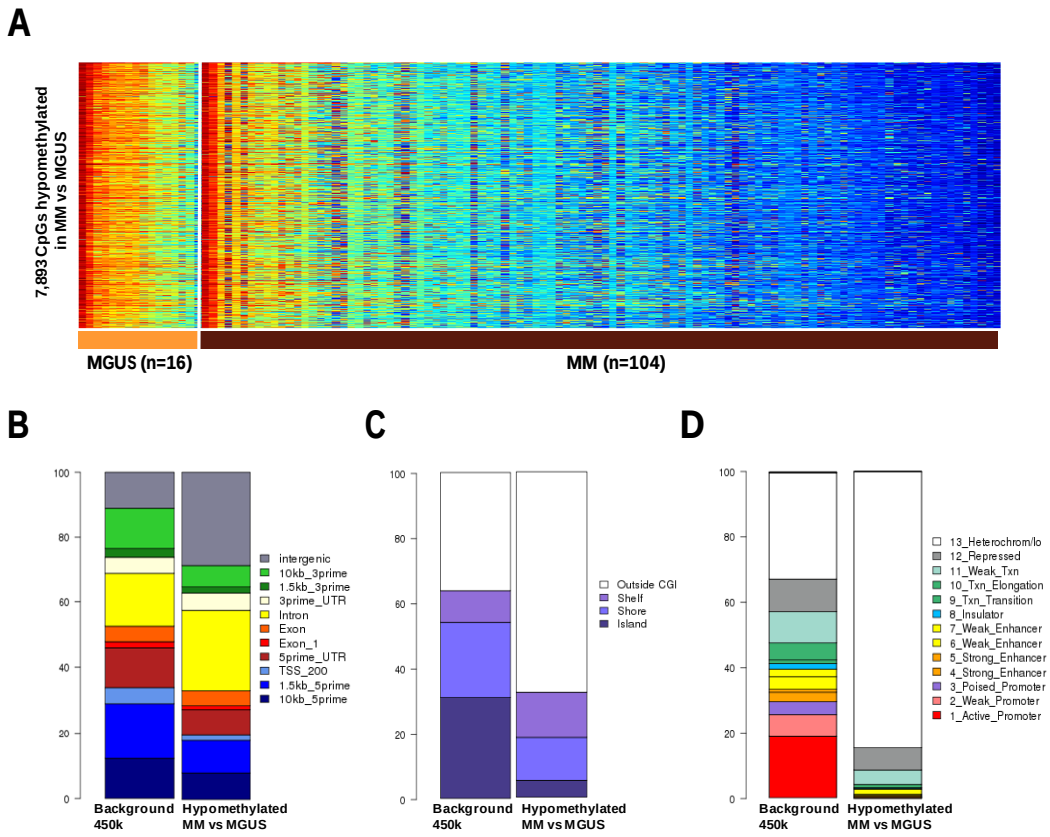


**Supplemental Fig. 3. Differential DNA methylation analysis between MM and MGUS.** (A) Heatmap of the 7,893 CpGs hypomethylated in MM vs. MGUS. Hypermethylated sites were not identified in MM vs MGUS. (B-D) Annotation of the hypomethylated CpGs in MM with regard to (B) gene-related regions, (C) CpG islands, shores or shelves and (D) chromatin states in IMBCs.

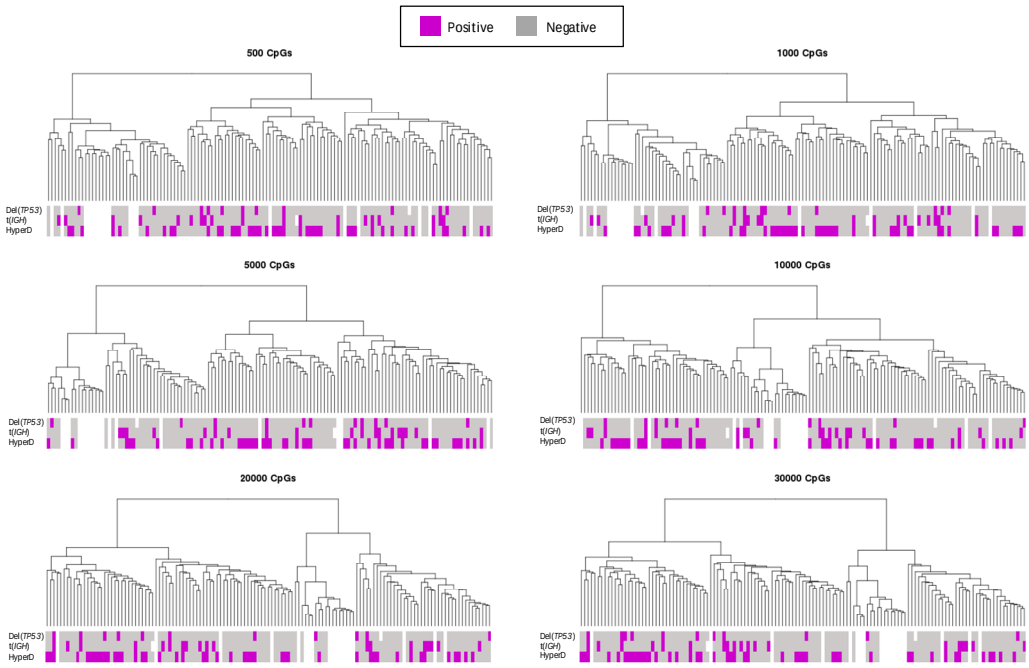


**Supplemental Fig. 4. Unsupervised hierarchical clustering of MM cases using different sets of variably methylated CpGs.** For these analyses, we used CpGs ranging from the top 500 CpGs to the top 30,000 CpGs with highest methylation variation among MM samples. This analysis shows that independently from the number of CpGs used, no association was identified between DNA methylation patterns and the different cytogenetic groups analyzed in our study.

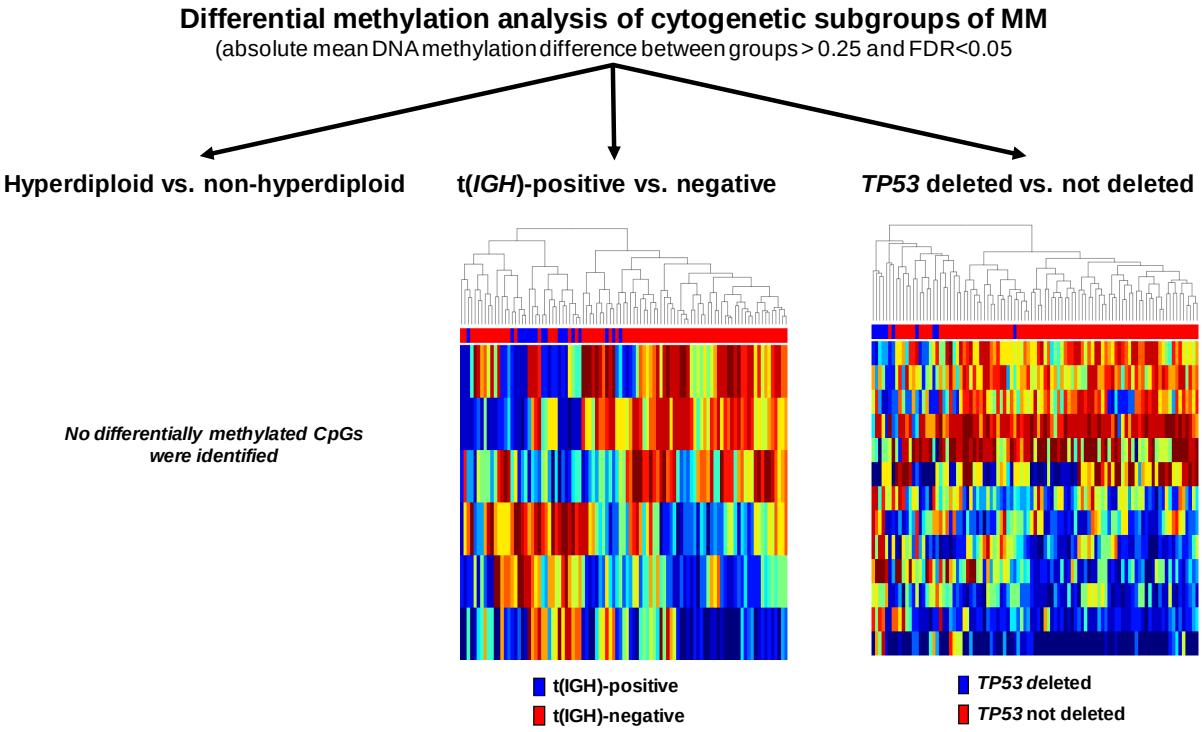


**Supplemental Fig. 5**. **Association between cytogenetics and DNA methylation signatures in MM**. (Left) No differentially methylated CpGs were observed between hyperdiploid versus non-hyperdiploid MM patient samples. (Middle) Hierarchical cluster analysis of CpGs differentially methylated in MM patient samples with *IGH* translocation versus samples without *IGH* translocation. (Right) Hierarchical cluster analysis of CpGs differentially methylated in MM patient samples with *TP53* deletion versus samples without *TP53* deletion.

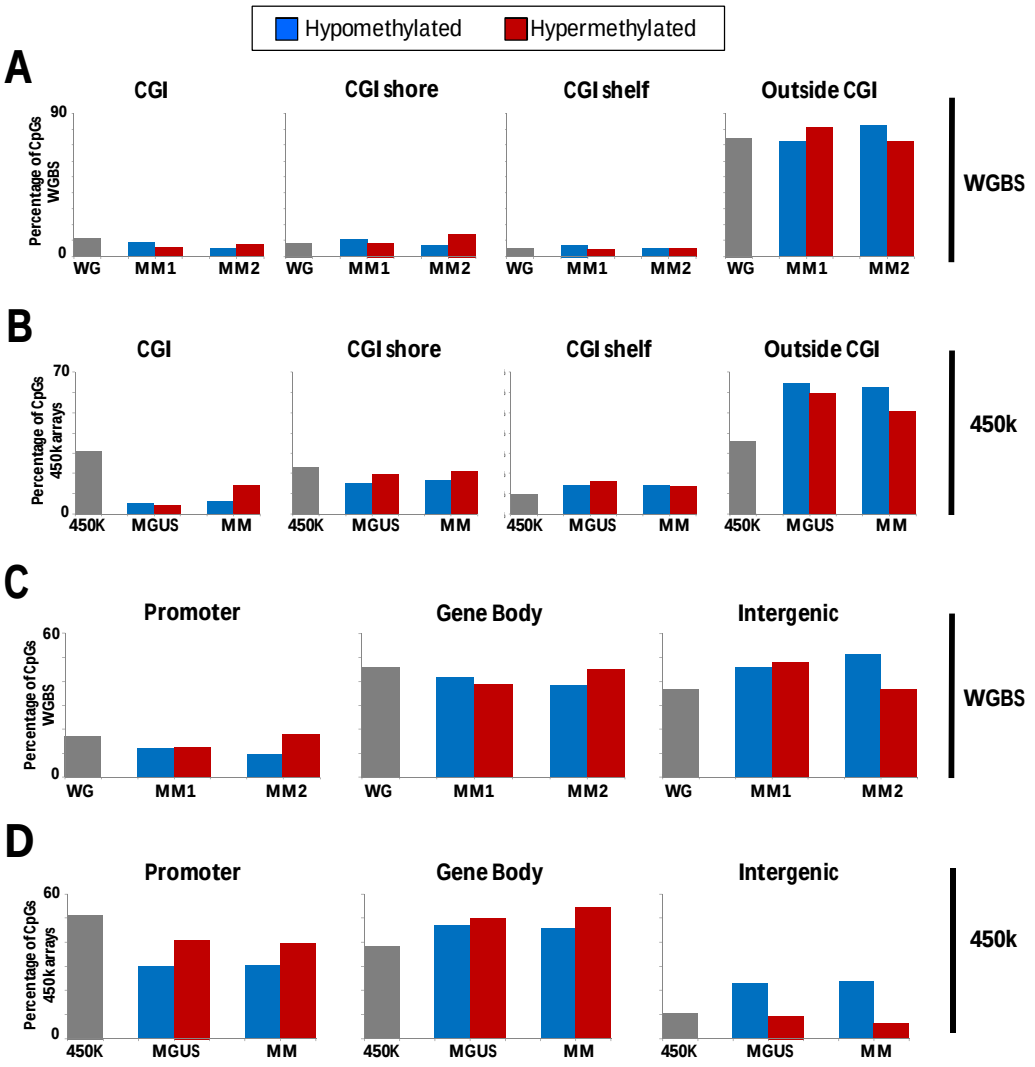


**Supplemental Fig. 6. Hypo- or hypermethylated CpGs in MM are associated with gene bodies and regions lacking CpG islands (CGIs)**. (A, B) Relative distribution of differentially hypo- or hypermethylated CpGs within CGIs, CGI shores (0–2 kb from island edge), CGI shelves (>2 to 4 kb from island edge) or outside CGIs using WGBS (A) or HumanMethylation450 BeadChip (B) data. (C, D) Relative distribution of differentially hypo- or hypermethylated CpGs across different gene-related regions using WGBS (C) or HumanMethylation450 BeadChip (D) data.

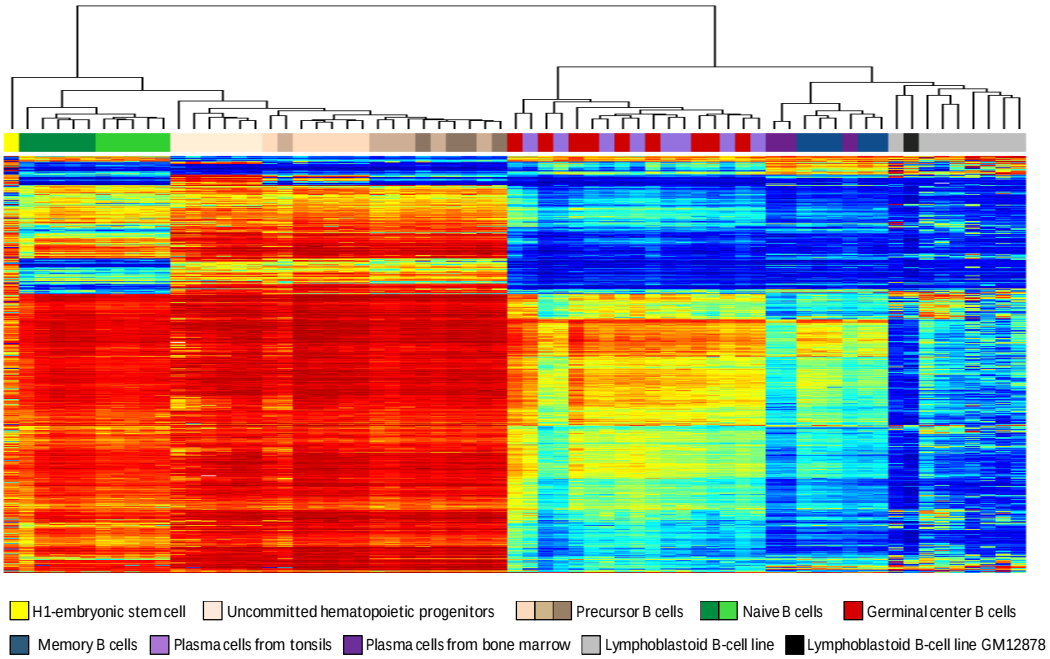


**Supplemental Fig. 7. Immortalized mature B cells (i.e. lymphoblastoid B-cell lines) show a DNA methylation profile similar to normal memory B cells and plasma cells**. Unsupervised hierarchical clustering analysis of CpGs with variable DNA methylation levels (SD >0.2) in lymphoblastoid B cell lines (including GM12878 and other cell lines), ESC cell line (H1) and sorted cells from multiple B-cell differentiation stages.

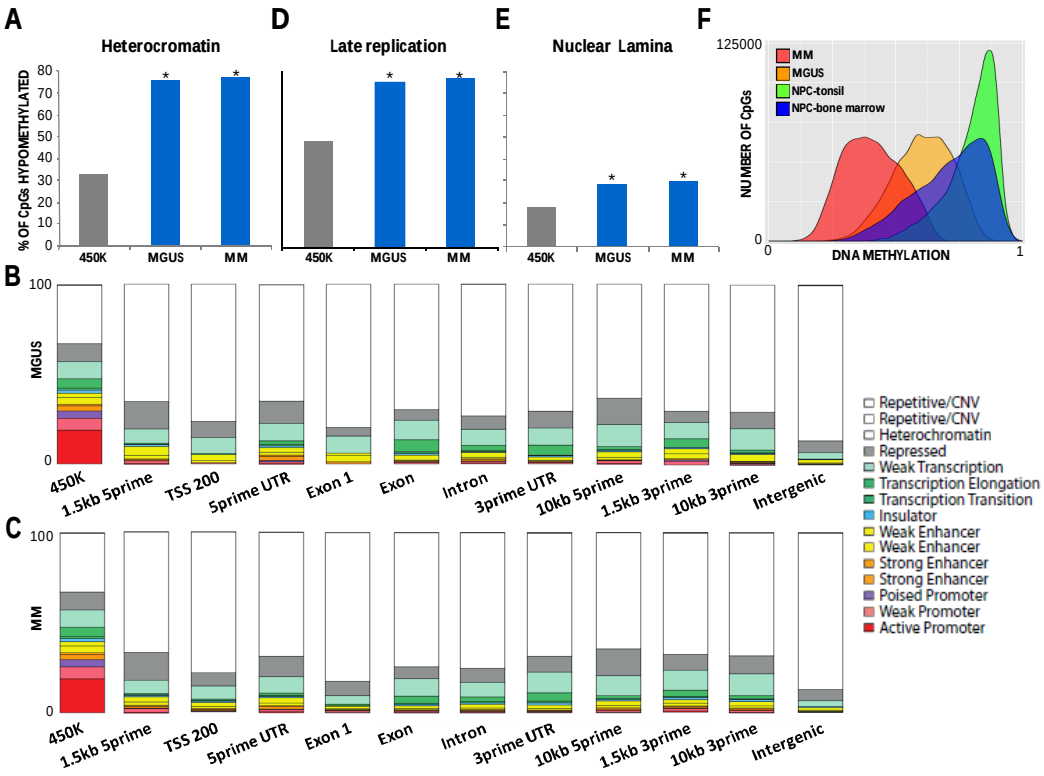


**Supplemental Fig. 8**. **Hypomethylated CpGs in plasma cell disorders are located in heterochromatic domains**. (A) Percentage of hypomethylated CpGs associated to heterochromatic regions in MGUS and MM patient samples using HumanMethylation450 BeadChip data. (B, C) Percentage of hypomethylated CpGs associated to heterochromatic regions in MGUS (B) and MM (C) patient samples across different gene-related regions. (D) Percentage of hypomethylated CpGs associated to late replication timing in MGUS and MM patient samples. (E) Percentage of hypomethylated CpGs associated to lamina-associated domains (LADs) in MGUS and MM patient samples. (F) DNA methylation levels of CpGs associated to LADs in MM, MGUS, normal plasma cells (NPCs) from tonsil and NPCs from bone marrow of healthy donors.TSS 200: 1-200 bp upstream of the transcription start site (TSS); UTR: untranslated region; 1.5kb 5prime: 1500 bp upstream of the 5´UTR; 10kb 5prime: 10000 bp upstream of the 5´UTR; 1.5kb 3prime: 1500 bp downstream of the 3´UTR; 10kb 3prime: 10000 bp downstream of the 3´UTR.

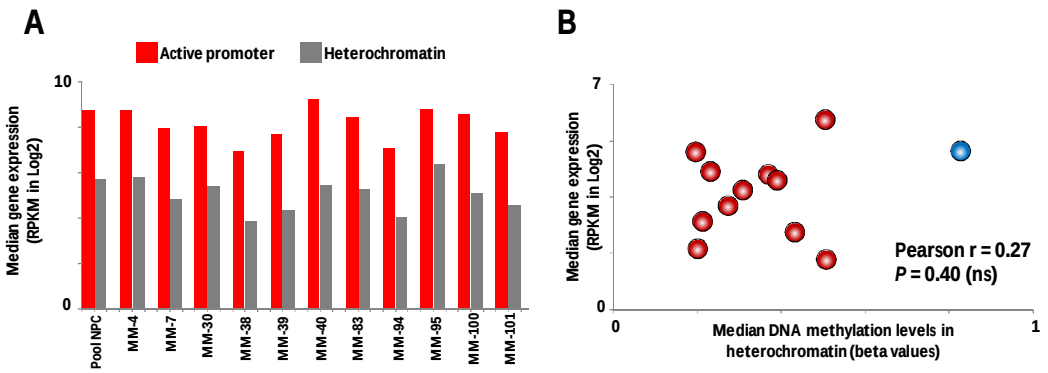


**Supplemental Fig. 9. Hypomethylation of heterochromatin in MM affects genes downregulated both in NPC and MM.** (A) Median expression of genes located in heterochromatic regions suffering hypomethylation in MM as compared to the expression levels of genes located in active promoters. (B) Scatter plot showing that the median methylation level of heterochromatin is independent from the median expression of the affected genes.

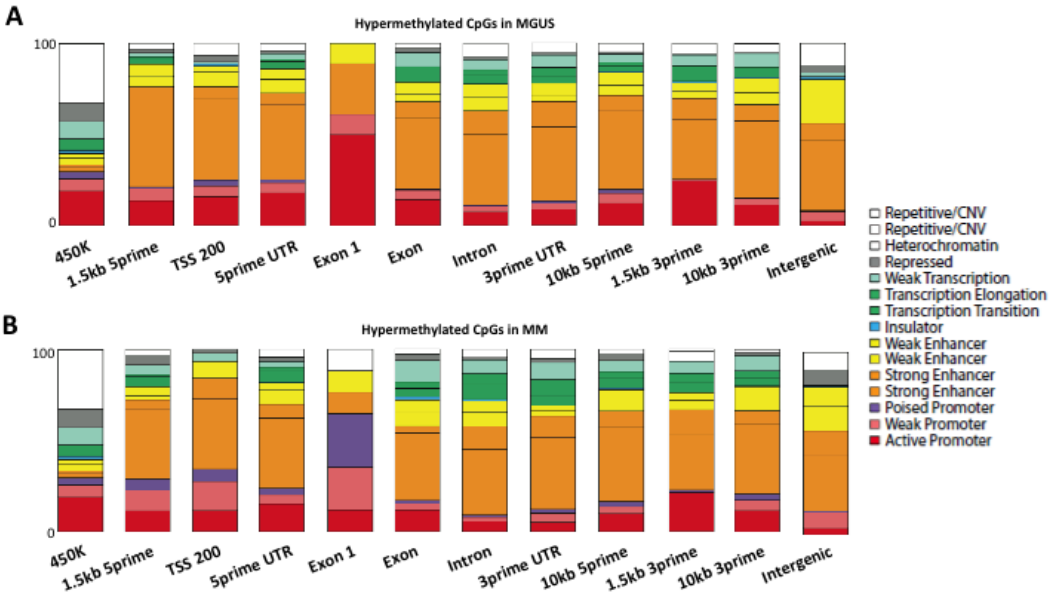


**Supplemental Fig. 10. Hypermethylated CpGs in plasma cell disorders are located in enhancer regions**. (A, B) Percentage of hypermethylated CpGs associated to enhancer regions in MGUS (A) and MM (B) patient samples across different gene-related regions.
TSS 200: 1-200 bp upstream of the transcription start site (TSS); UTR: untranslated region; 1.5kb 5prime: 1500 bp upstream of the 5´UTR; 10kb 5prime: 10000 bp upstream of the 5´UTR; 1.5kb 3prime: 1500 bp downstream of the 3´UTR; 10kb 3prime: 10000 bp downstream of the 3´UTR.

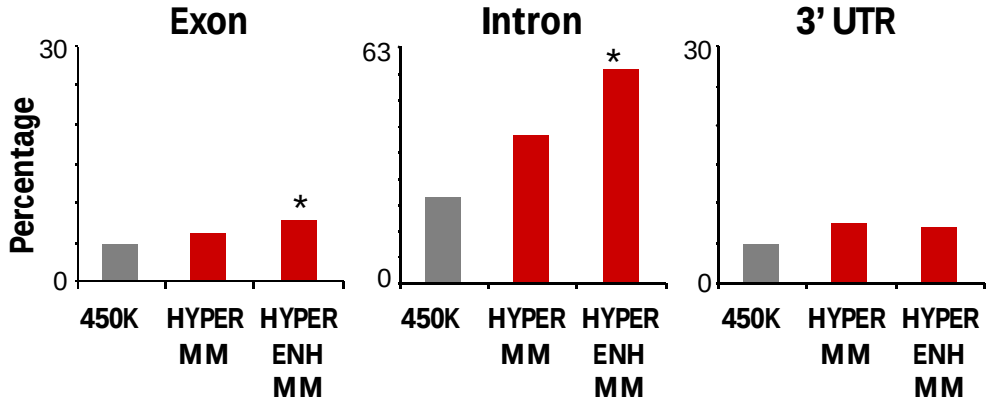


**Supplemental Fig. 11. Enhancer-associated CpGs hypermethylated in MM are enriched in intronic regions**. Relative distribution of hypermethylated CpGs in MM (HYPER MM) and enhancer-associated hypermethylated CpGs in MM patient samples (HYPER ENH MM) in exons (left), introns (middle) and 3' UTR regions (right). *: P<0.

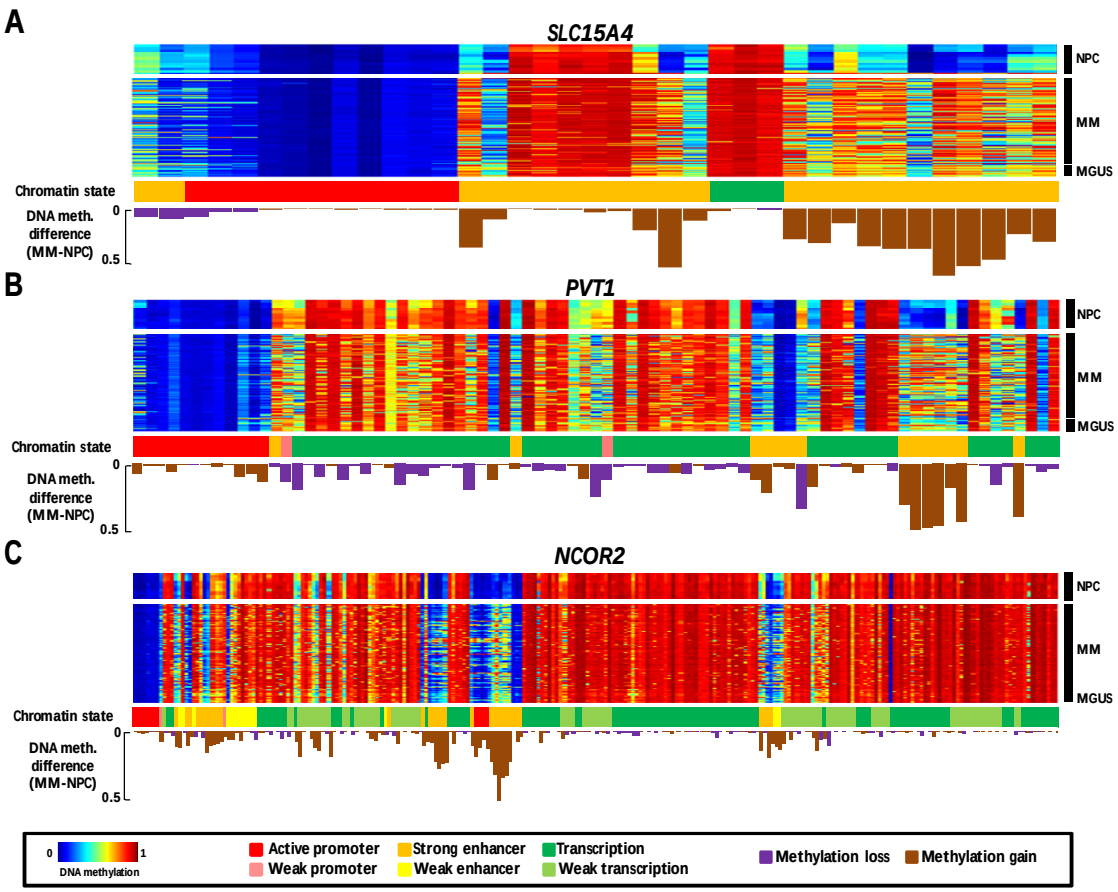


**Supplemental Fig. 12. DNA methylation landscape of the three genes shown in Fig. 3.** This analysis shows that hypermethylation takes place in active enhancer elements and not in promoter regions. Sequential CpGs measured by HumanMethylation450 BeadChip are shown, the 5' promoter region is on the left whereas the 3' region of the gene is located on the right.

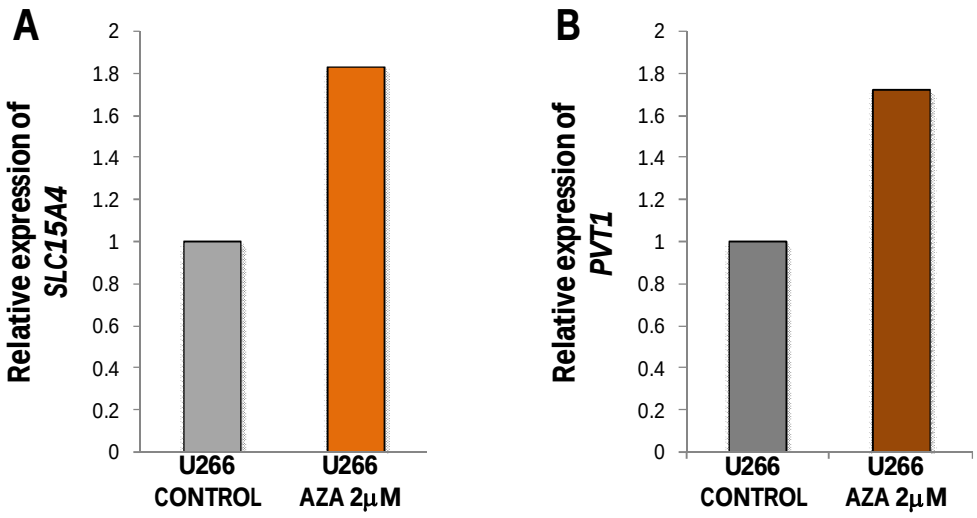


**Supplemental Fig. 13. Gene expression after 5-azacytidine treatment.** U266 cell line was treated with 2μM of 5-azacytidine during 72 hours. Gene expression of (A) *SLC15A4* and (B) *PVT1* genes was analyzed by Q-RT-PCR. AZA: 5-azacytidine.

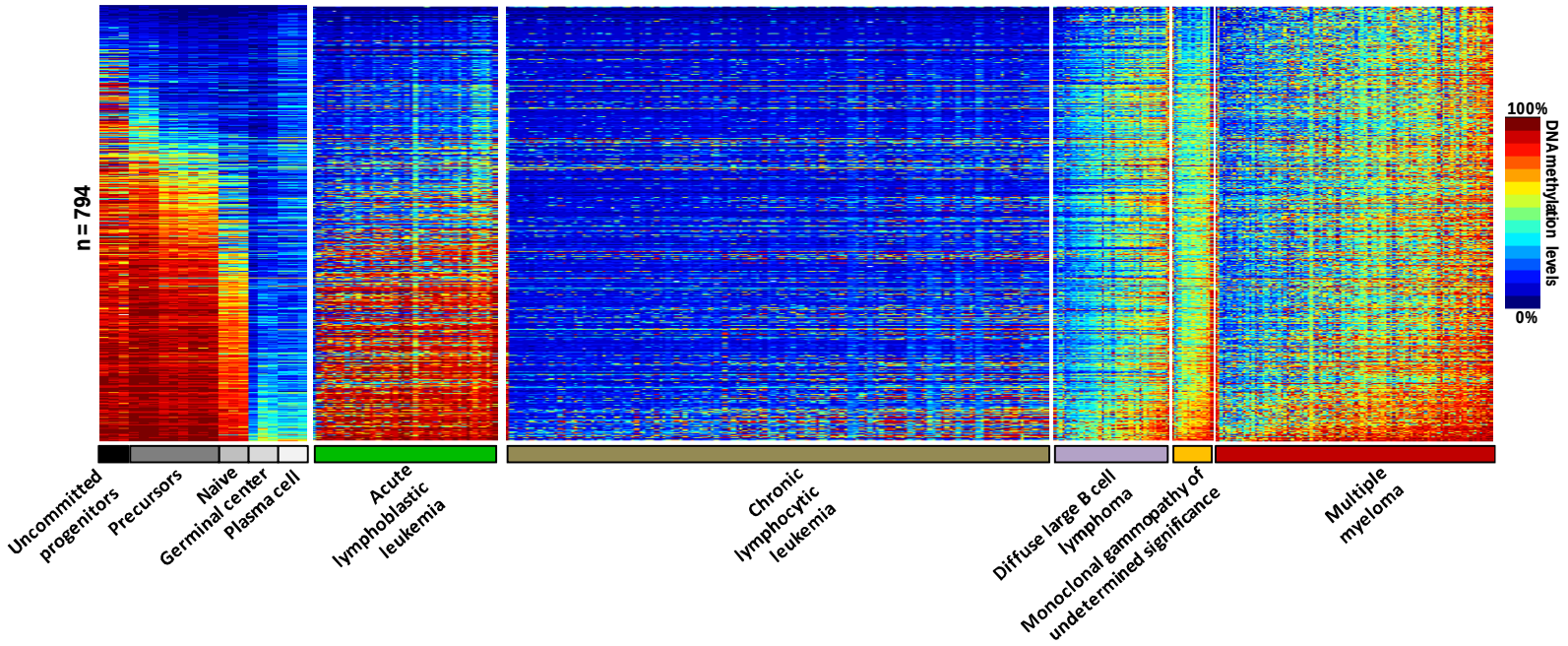


**Supplemental Fig. 14. DNA methylation status of hypermethylated enhancers in MM and in other B-cell neoplasms.** Depicted are the DNA methylation levels of enhancer-associated CpGs in several B-cell differentiation stages and B-cell malignancies.

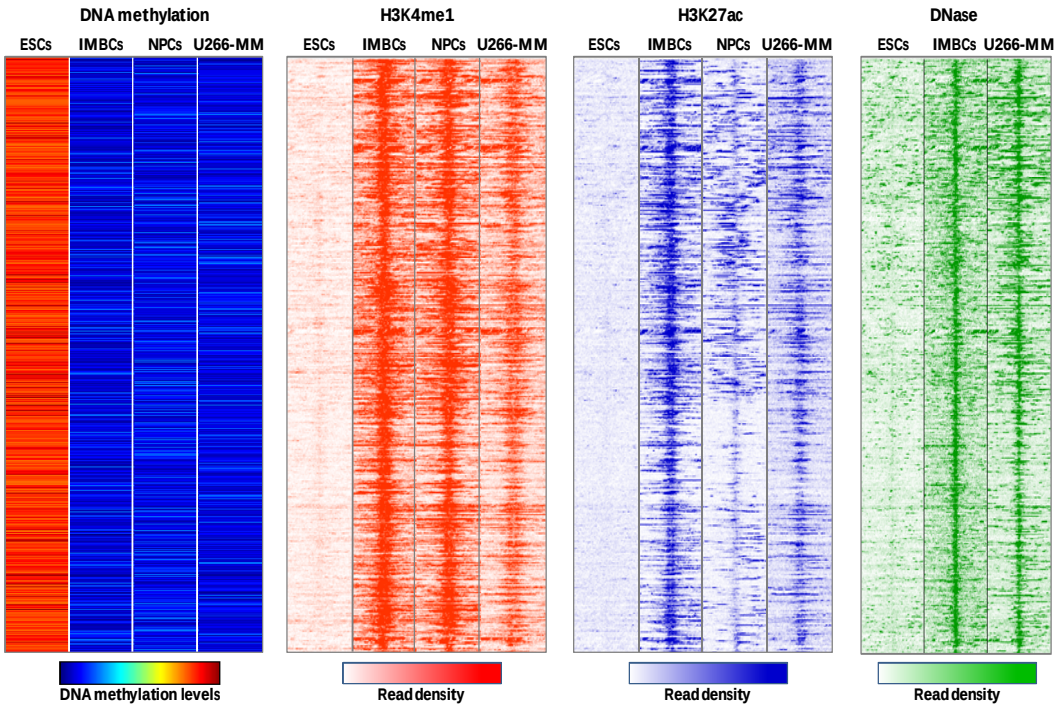


**Supplemental Fig. 15**. **Chromatin architecture of enhancer regions hypomethylated in IMBCs and MM**. To support the validity of the data shown in Fig. 4B, we selected 1,994 CpGs located in unmethylated enhancers in IMBCs and NPCs that remain unmethylated in MM, but are methylated in ESCs. This analysis clearly shows that the unmethylated status of CpGs is associated with chromatin features specific for active enhancers whereas methylated CpGs in ESCs is related to enhancer inactivation. This finding further confirms that *de novo* hypermethylation in MM is associated with enhancer decommissioning.

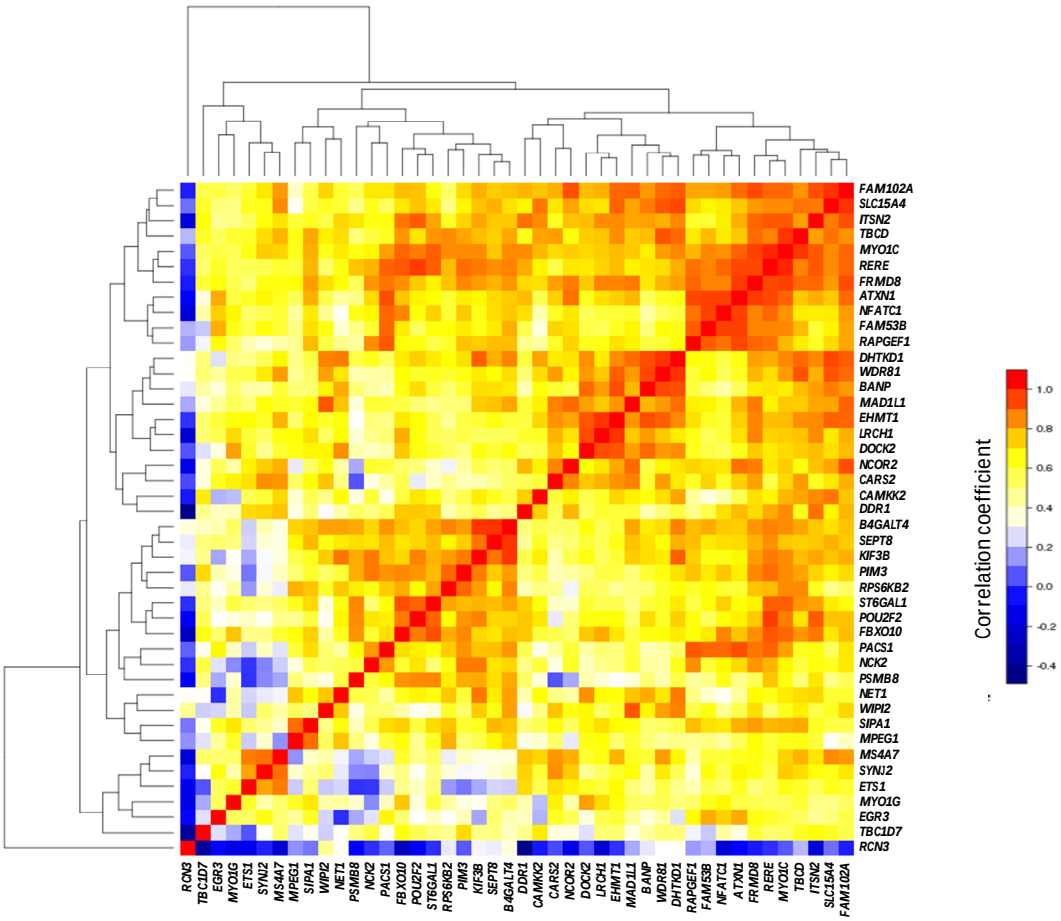


**Supplemental Fig. 16**. **Correlation matrix of expression levels in MM cases**. This matrix includes the genes with the highest association between enhancer methylation and gene expression.

## Supplemental Tables

(note: only small tables are shown here, larger tables have been submitted as individual files in excel format)

**Supplemental Table 2.** Sequencing amounts in each of the three samples analyzed by WGBS.

| Sample name | Yield passing filter (Gb) | Mapping (%) | Unique mapping (%) | Mean coverage |
|---|---|---|---|---|
| NPC | 183.452 | 95.0 | 82.1 | 55.5 |
| MM1 | 184.799 | 94.6 | 80.2 | 55.7 |
| MM2 | 175.627 | 92.7 | 78.4 | 51.9 |

NPC: normal plasma cells; MM: multiple myeloma; WGBS: whole-genome bisulfite sequencing

**Supplemental Table 5.** Primers and conditions used to amplify selected hypermethylated enhancer regions.

| Gene | Technique | | Primers | Sequence | Annealing Temperature | Amplification Length |
|---|---|---|---|---|---|---|
| **NCOR2** | Luciferase Reporter Assay | | NCOR2-F | ***GGATCC*** TCATAGCTAATGCCCAGCAC | 59 | 376bp |
| | | | NCOR2-R | ***AAGCTT*** GTGGGGGTGGGGAGTCTT | | |
| **PVT1** | Luciferase Reporter Assay | | PVT1-F | ***GGATCC*** GTGGATGTATGAGCCGATCC | 60 | 350bp |
| | | | PVT1-R | ***AAGCTT*** CCTCTTCTGACTTGGCATGG | | |
| **SLC15A4** | Luciferase Reporter Assay | | SLC15A4-F | ***GGATCC*** ATCCCCCTTTCACAGAGGTC | 59 | 376bp |
| | | | SLC15A4-R | ***AAGCTT*** AGGAGCAGAAAATGGAGCAA | | |
| | Pyrosequencing | Amplification | Universal-F | GTGACGTACTAGCAACG | 57 | |
| | | | Universal-R | [bio]TAGCAGGATACGACTATC | | |
| **NCOR2** | Pyrosequencing | Amplification | NCOR2-BP-F | ***GTGACGTACTAGCAACG*** TTAGTATTTATTGTTTATAAGGTAGG | 51 | 362bp |
| | | | NCOR2-BP-R | ***[bio]TAGCAGGATACGACTATC*** TAAAAATAAAAAATCTTAACAAC | | |
| | | Sequencing | NCOR2-PYR-1 | GTATAGGGAGGGTAATAGAT | | |
| | | Sequencing | NCOR2-PYR-2 | TGTGTGATTTTTTTTATAGT | | |
| **PVT1** | Pyrosequencing | Amplification | PVT1-BP-F | ***GTGACGTACTAGCAACG*** TGGGATTAGTTTTTTTATTTGATGG | 59 | 257bp |
| | | | PVT1-BP-R | ***[bio]TAGCAGGATACGACTATC*** AAACTCTCCACACATTTCTCCTAAC | | |
| | | Sequencing | PVT1-PYR-1 | ATTTGTTGGGGTTTGGGTTT | | |
| | | Sequencing | PVT1-PYR-2 | TTTGAAGAAAGAGGAAG | | |
| **SLC15A4** | Pyrosequencing | Amplification | SLC15A4-BP-F | ***GTGACGTACTAGCAACG*** GAGGTTTGGAATTGTTTATTTTGTAAA | 55 | 347bp |
| | | | SLC15A4-BP-R | ***[bio]TAGCAGGATACGACTATC*** AACAACTTAATTCCAAAACACTC | | |
| | | Sequencing | SLC15A4-PYR-1 | TATTATTATTTAATGTGTAG | | |
| | | Sequencing | SLC15A4-PYR-2 | TGTTTTTGTTATTATG | | |

**Supplemental Table 6.** Gene Ontology analysis of Hypermethylated Enhancers in MM.

| GO Term | Description | P-value | FDR q-value | Fold enrichment |
|---|---|---|---|---|
| GO:0030183 | B cell differentiation | 6.27E-06 | 5.57E-03 | 5.87 |
| GO:0002263 | cell activation involved in immune response | 4.68E-06 | 4.92E-03 | 4.96 |
| GO:0002366 | leukocyte activation involved in immune response | 4.68E-06 | 5.41E-03 | 4.96 |
| GO:0038094 | Fc-gamma receptor signaling pathway | 5.61E-05 | 1.91E-02 | 4.61 |
| GO:0038096 | Fc-gamma receptor signaling pathway involved in | 5.61E-05 | 1.96E-02 | 4.61 |
| GO:0002433 | immune response-regulating cell surface receptor signaling pathway involved in phagocytosis | 5.61E-05 | 2.02E-02 | 4.61 |
| GO:0002431 | Fc receptor mediated stimulatory signaling pathway | 6.35E-05 | 1.98E-02 | 4.54 |
| GO:0038093 | Fc receptor signaling pathway | 8.08E-05 | 2.39E-02 | 4.42 |
| GO:0042113 | B cell activation | 9.08E-06 | 6.55E-03 | 4.32 |
| GO:0030098 | lymphocyte differentiation | 6.63E-05 | 2.02E-02 | 3.4 |
| GO:0002429 | immune response-activating cell surface receptor signaling pathway | 4.82E-05 | 1.86E-02 | 3.17 |
| GO:0046649 | lymphocyte activation | 2.46E-06 | 3.55E-03 | 3.03 |
| GO:0002768 | immune response-regulating cell surface receptor signaling pathway | 9.85E-05 | 2.71E-02 | 2.98 |
| GO:0045321 | leukocyte activation | 1.14E-05 | 6.95E-03 | 2.63 |
| GO:0051249 | regulation of lymphocyte activation | 8.44E-05 | 2.44E-02 | 2.49 |
| GO:0000122 | negative regulation of transcription from RNA polymerase II promoter | 2.02E-05 | 9.32E-03 | 2.17 |
| GO:0001775 | cell activation | 5.61E-05 | 1.85E-02 | 2.09 |
| GO:0051253 | negative regulation of RNA metabolic process | 6.25E-06 | 6.01E-03 | 1.93 |
| GO:0045892 | negative regulation of transcription, DNA-dependent | 1.04E-05 | 7.09E-03 | 1.93 |
| GO:0009890 | negative regulation of biosynthetic process | 3.79E-06 | 4.86E-03 | 1.86 |
| GO:0002682 | regulation of immune system process | 1.41E-05 | 7.74E-03 | 1.85 |
| GO:0035556 | intracellular signal transduction | 2.49E-07 | 1.44E-03 | 1.83 |
| GO:0010558 | negative regulation of macromolecule biosynthetic process | 1.22E-05 | 7.02E-03 | 1.83 |
| GO:0031327 | negative regulation of cellular biosynthetic process | 1.04E-05 | 6.70E-03 | 1.82 |
| GO:0051172 | negative regulation of nitrogen compound metabolic process | 1.73E-05 | 8.34E-03 | 1.82 |
| GO:0045934 | negative regulation of nucleobase-containing compound metabolic process | 2.40E-05 | 1.06E-02 | 1.81 |
| GO:2000113 | negative regulation of cellular macromolecule biosynthetic | 3.21E-05 | 1.32E-02 | 1.81 |
| GO:0010629 | negative regulation of gene expression | 9.82E-05 | 2.77E-02 | 1.76 |
| GO:0031324 | negative regulation of cellular metabolic process | 1.51E-05 | 7.92E-03 | 1.67 |
| GO:0010605 | negative regulation of macromolecule metabolic process | 2.47E-05 | 1.05E-02 | 1.65 |
| GO:0009892 | negative regulation of metabolic process | 1.54E-05 | 7.73E-03 | 1.64 |
| GO:0002376 | immune system process | 3.98E-05 | 1.58E-02 | 1.61 |
| GO:0007166 | cell surface receptor signaling pathway | 7.83E-06 | 6.46E-03 | 1.55 |
| GO:0048523 | negative regulation of cellular process | 8.33E-07 | 1.60E-03 | 1.48 |
| GO:0048519 | negative regulation of biological process | 5.06E-07 | 1.46E-03 | 1.47 |
| GO:0048583 | regulation of response to stimulus | 4.96E-05 | 1.85E-02 | 1.45 |
| GO:0007165 | signal transduction | 1.10E-06 | 1.81E-03 | 1.41 |
| GO:0051716 | cellular response to stimulus | 8.12E-06 | 6.26E-03 | 1.33 |
| GO:0050794 | regulation of cellular process | 3.22E-07 | 1.24E-03 | 1.24 |
| GO:0050896 | response to stimulus | 6.22E-05 | 2.00E-02 | 1.24 |
| GO:0050789 | regulation of biological process | 2.25E-07 | 2.60E-03 | 1.23 |
| GO:0065007 | biological regulation | 8.21E-07 | 1.90E-03 | 1.21 |

**Supplemental Table 8.** Correlation between de expression of B-cell transcription factors and methylation levels of B-cell enhancers hypermethylated in Multiple Myeloma.

| Transcription factor | Pearson Correlation Coefficient | *P* value |
|---|---|---|
| STAT5A | -0.79 | 0.002 |
| PAX5 | -0.73 | 0.007 |
| NFATC1 | -0.71 | 0.009 |
| BATF | -0.62 | 0.032 |
| EBF1 | -0.57 | 0.052 |
| IRF4 | -0.51 | 0.091 |
| P300 | -0.45 | 0.137 |
| ZNF217 | -0.43 | 0.163 |
| CHD2 | -0.41 | 0.184 |
| POU2F2 | -0.4 | 0.19243 |
| STAT3 | -0.38 | 0.22835 |
| BCL11A | -0.37 | 0.23984 |
| ESR1 | -0.36 | 0.25702 |
| MTA3 | -0.36 | 0.25583 |
| SP1 | -0.3 | 0.33955 |
| MEF2A | -0.29 | 0.36048 |
| SPI1 | -0.29 | 0.36893 |
| FOXM1 | -0.28 | 0.3751 |
| WRNIP1 | -0.28 | 0.38023 |
| ATF2 | -0.26 | 0.4057 |
| TBL1XR1 | -0.26 | 0.41666 |
| IKZF1 | -0.24 | 0.45734 |
| BCL3 | -0.22 | 0.50197 |
| BHLHE40 | -0.19 | 0.55664 |
| PBX3 | -0.19 | 0.5605 |
| USF2 | -0.19 | 0.54512 |
| CEBPB | -0.16 | 0.61473 |
| TCF12 | -0.15 | 0.64636 |
| JUN | -0.14 | 0.67096 |
| FOS | -0.13 | 0.67608 |
| MEF2C | -0.13 | 0.67594 |
| RUNX3 | -0.12 | 0.71466 |
| FOSL1 | -0.11 | 0.73252 |
| BCLAF1 | -0.08 | 0.80327 |
| PML | -0.02 | 0.95788 |
| SMC3 | -0.02 | 0.95181 |
| TCF3 | 0.02 | 0.95303 |
| EGR1 | 0.18 | 0.56879 |
| GATA2 | 0.19 | 0.5542 |
| NFIC | 0.34 | 0.27599 |
| FOSL2 | 0.38 | 0.22096 |